Green Synthesis of Gold Nanoparticles (AuNPs) from Plants

Subjects: Agriculture, Dairy & Animal Science
Contributor: Dr. Siddhartha Pati

Gold nanoparticles (AuNPs) are becoming promising cancer therapeutic and diagnostic metal NPs that attract researchers due to their unique physiochemical properties such as stability, biocompatibility, high thermal activity, optical, electrical, high surface area to volume ratio surface chemistry, and multifunctionalization, etc. By fine tuning the components and concentrations, AuNPs can be easily manufactured into various forms and sizes. AuNPs have also shown significant advancement in treating inflammatory diseases and bacterial infections.

Keywords: gold nanoparticles ; AuNPs ; green synthesis ; anticancer ; plants ; therapy

1. Properties of Gold Nanoparticles

To synthesize stable nanoparticles (NPs), gold (Au) is regarded as suitable metal. Most of the physical properties of inorganic nanoparticles are found to be dependent on the size and shape of the NPs. The gold nanoparticles (AuNPs) have wide applications in different fields due to their specific optical and physical properties. AuNPs possess significant properties, such as (a) small size (1–100 nm), (b) physical and chemical properties based on size, shape, and composition, (c) excellent robustness, (d) qualitative and quantitative target binding ability, etc. [1].

1.1. Shape and Size

There are various methods for the synthesis of AuNPs having different shapes and sizes. The size and shape of AuNPs are the two primary parameters that control the chemical, physical and electrocatalytic properties of gold nanoparticles. Metal nanoparticles in the size range of 1–10 nm have size-dependent properties compared to bulk materials [2]. There are very few methods for the production of AuNPs with uniform sizes. Michael Faraday introduced the two-phase system to prepare AuNPs by reducing gold salt by phosphorous in carbon disulphide for the first time. Researchers have developed a popular method for synthesising smaller AuNPs. They reduced gold salt by sodium borohydride in the presence of the capping agent dodecanethiol [3]. They confirmed the size of the NPs in the range 1–3 nm using HRTEM (High-Resolution Transmission Electron Microscopy). It is possible to control the size of NPs by varying the concentration of thiols. G. Frens agreed with Turkevich's data that reduction of gold chloride salt using sodium citrate solution is an efficient method to prepare monodispersed gold nanoparticles of different diameters. By changing the ratio of reactants, independent nucleation and growth of metal nanoparticles with different diameters can be achieved [4][5]. The size of AuNPs are tuneable through the alteration of gold precursor and reducing the power of reducing agents. It is observed that strong reducing agents, such as $NaBH_4$ offer the synthesis of small size AuNPs and weaker reducing agents, such as citrate, resulted in comparatively larger NPs. Researchers have investigated the effect of chloride ion concentration on the size of AuNPs via citrate reduction. They find that size of gold NPs are caused by the aggregation of gold NPs induced by chloride ions [6]. In a typical synthesis, chloroauric acid ($HAuCl_4$) is reduced by 5% sodium citrate solution at room temperature. The chloride ion concentration is varied using different concentrations of NaCl solutions. They performed the same experiment using $NaBH_4$ as a reductant, and the interesting results are placed in **Table 1**. The table includes the data for the effect of different concentrations of NaCl on the size of AuNPs in the presence of different reactants such as sodium citrate and sodium borohydride, respectively. With an increase in NaCl concentration from 1 to 20 mM, the UV-visible absorption maxima (max) are also shifted towards higher wavelengths that indicate an increased size of AuNPs.

Table 1. The effect of Cl^- ion concentration and reductant on AuNPs size.

	Concentration of NaCl (mM)	UV-Visible Absorption Maxima [λ_{max} (nm)]	Size Ranges from TEM (nm)
$HAuCl_4$ (0.25 mM) + 5% Sodium citrate (Both the reactants are in 5:1 ratio)	1	517	19 nm (±7)
	5	520	25 nm (±11)
	10	525	38 nm (±21)
	15	528	40 nm (±31)
	20	531	47 nm (±36)
$HAuCl_4$ (0.25 mM) + Sodium borohydride ($NaBH_4$)	0	490	3
	20	520	12

Solvents used in the synthesis of NPs play an important role as either interaction between nanoparticle surface and solvent molecule or solvent and ligand molecules direct its final size and morphology [7][8]. Scholars have challenged the two-phase synthesis of NPs by Brust and co-workers and developed a single-phase synthesis of monodispersed gold nanoparticles using borane complexes as a reductant in organic solvents. In a typical process, $AuPPh_3Cl$ (0.25 mmol) and dodecanethiol (0.125 mmol) is mixed with benzene, and 2.5 mmol solution of the tert-butylamine-borane complex is added as reductant that forms 6.2 nm size gold nanoparticles [9]. In a modified Stucky's method, Song and coworkers have prepared mono dispersed AuNPs from the reaction of $AuPPh_3Cl$ with an amine borane complex tert-butylamine borane (TBAB) having thiol ligand. In the absence of thiol, the AuNPs are found to have polydispersity, while in the presence of thiol, the synthesized NPs are monodispersed, having a size of 5.0 nm ± 0.4 nm [10]. To synthesize large size AuNPs, the seeded growth method is preferred. In this method, small size gold nanoparticles have been synthesized that act initially as seeds for the growth of larger gold nanoparticles. Then, separation of nucleation and growth of the NPs, we may increase the size of AuNPs up to 300 nm [2][11]. Stanglmair and co-workers have reported synthesizing monodispersed AuNPs with 20 nm average diameter in size via the seeded growth method. They synthesized gold nanoparticles of 9 nm size, in toluene as solvent and oleylamine as reductant cum stabilizing agent, were further used as a seed to produce AuNPs of 20 nm average size. Researchers have reported the synthesis of spherical shape AuNPs from $H[AuCl_4]\cdot 3H_2O$ as a precursor, ascorbic acid as reductant and sodium citrate as a stabilizer. In the first step, they were able to synthesize NPs with 30 nm size, which then acts as a seed for the production of AuNPs, having 69 nm and 118 nm sizes and even further growth [12]. The report shows that AuNPs with different sizes and shapes, such as long nanorods, short nanorods, cubes and spheres can be prepared via reversible flocculate formation surfactant micelle-induced depletion interaction. To obtain different shapes of NPs, the tuning of surfactant concentration and extraction of flocculates from the sediment are important steps [13]. Jianhui Zhang, with his co-workers, has investigated the shape-selective synthesis of AuNPs with controlled size and different shapes, such as hexagons, belts, rods, triangles, octahedrons and dumbbells. In the process, water molecules are attached with poly(vinylpyrrolidone) (PVP) and *n*-pentanol to form a two-phase system of water/PVP/n-pentanol (WPN). PVP can act as a reductant and stabilizer where the presence of water can modify the reducing ability of PVP. However, they utilized PVP as a capping agent rather than a reductant. They have observed the region-selective distribution of water and PVP in the WPN system, which offers kinetically controlled growth of novel AuNPs nanostructures [14]. Researchers have studied the effect of temperature on the size of AuNPs by synthesizing gold nanoparticles varying temperature using tetraoctylammonium bromide (TOAB) as a stabilizer. The room temperature synthesis confirms AuNPs with an average size of 5.2 nm having a spherical shape. When the annealing of the AuNPs synthesis was performed at 100 °C for 30 min, a drastic change in the shapes of the gold nanoparticles was observed. The sizes of nanoparticles change from 5.2 nm to 6 nm, bearing shapes such as hexagons, pentagons, and squares under HRTEM observation, whose corresponding three-dimensional shapes are cuboctahedron, icosahedron, and a cube, respectively. On annealing, at 200 °C, the morphology, as well as size of AuNPs, changed drastically. The HRTEM shows the average size of the NPs to be 15 nm with different shapes, such as hexagon, triangle and pentagons. Similarly, nanoparticles and nanocubes are obtained when annealing is performed at 300 °C [15]. An interesting process, called the dewetting process, has attracted the researcher in the synthesis of nanoporous AuNPs. In this method, Au/Ag bilayer alloy film is initially produced, where AuNPs are much smaller in comparison to silver nanoparticles (AgNPs). Then, AgNPs are removed by treating the Au/Ag bilayer in 65 wt% HNO_3 solution at 21 °C, called dealloying. After dealloying, Au (5 nm)/Ag (20 nm) bilayer AuNPs with 274 nm are found, while Au (10 nm)/Ag (20 nm) bilayer-formed AuNPs have a diameter of 307 nm [16]. Researchers have reported the synthesis of cap-shaped AuNPs with 110 nm size by evaporating gold adsorbed on polystyrene [17]. The atom-transfer radical polymerisation (ATRP) is a technique used by scholars to prepare monodispersed nanoparticles that might be useful for synthesizing NPs of other precursors [18]. Researchers have prepared gold nanoclusters in the size range 7–20 nm having positive and negative charges in presence of polyamidoamine dendrimers (PAMAM) or sodium citrate [19]. Luca and co-workers have synthesized gold nanostar (AuNS) from $HAuCl_4$ as a precursor using hydroxylamine as a reductant above pH 11 maintained by HaOH solution. AuNS are formed in the pH range 12–12.5 where below pH 11, no reduction occurs

to Au (III) species. Thus, pH plays an important role in the size and morphology determination of AuNPs [20]. The graphical abstract presented in **Figure 2** tries to include varieties of available shapes for AuNPs.

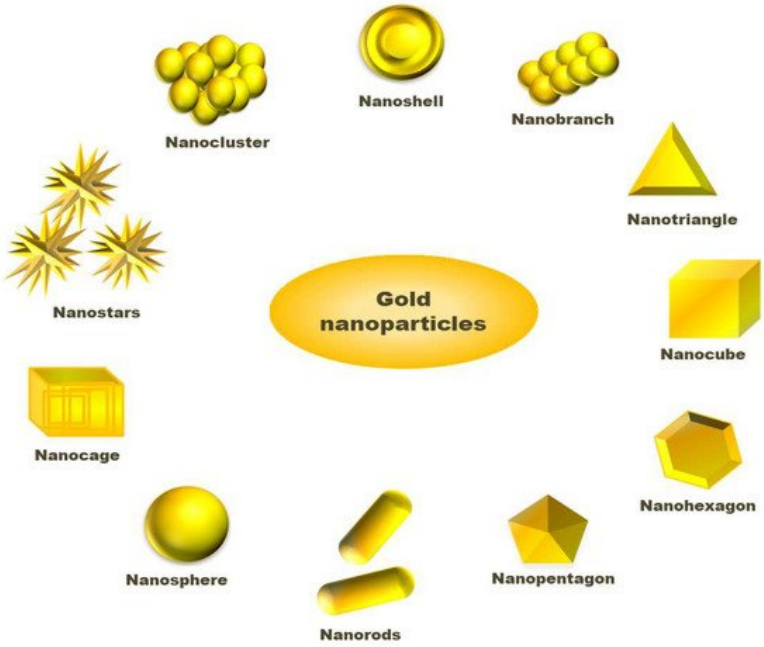

Figure 2. Different shapes available for gold nanoparticles.

1.2. Optical Properties

Nanoparticles possess excellent optical properties that are different from individual molecules and bulk metals. The optical properties of AuNPs related to surface plasmon resonance (SPR) are one of the reasons behind the vast success of AuNPs in nanoscience and technology [21]. As NPs are exposed to light, the oscillating electromagnetic field of light automatically induces collective coherent oscillation in the free electrons present in the conduction band of NPs. This eventually results in the charge separation that forms a dipole oscillation in the electric field of light. The amplitude of this oscillation reaches the zenith of maximum at a particular frequency known as surface plasmon resonance (SPR). The extent of SPR can be measured using a UV-visible spectrophotometer as the SPR absorbance for nanomaterials is much stronger than other metals. As per Mie theory, the SPR band intensity and wavelength depend upon factors, such as metal type, size, shape and structure of NPs, composition, and dielectric constant of the medium [22]. For gold nanorods, the PA spectra are found to split into two modes, namely transverse and longitudinal. It is interesting to note that gold Nanospheres having size ~20 nm in diameter have a characteristic strong PA absorption band centred at ~522 nm while for nanorods, there was observed a two-band centred at ~522 nm and ~698 nm for transverse and longitudinal SPR. The gold nanoparticles of size < 2 nm in diameter do not show such absorption [23]. The longitudinal SPR (LSPR) of such branched nanostructure is well understood with the help of the plasmon hybridisation model (PH). This method calculates the LPSR of complex structures, assuming it to be the result of LPSR of simpler structures [24]. Optical transmission spectroscopy can be employed to study surface plasmon excitation for two identical interacting spherical AuNPs. Researchers have studied SPR for three pairs of AuNPs with sizes 450 nm, 300 nm and 150 nm in interaction. It is found that, with a decrease in the inter-particle distance, red shifts in SPR are observed, while blue shift is found for orthogonal polarisation [25]. AuNPs can enhance the Raman signal from 10^6 to 10^{15} when exposed p monochromatic light. This phenomenon is called the surface-enhanced Raman scattering (SERS) technique that can be applied to distinguish tumour cells, mark tumour cells, or monitor tumour metabolism. AuNPs contain radioactive atoms that help in achieving desired radioactivity for treatment.

1.3. Electrical Properties

The semiconductor industries believe that complementary metal-oxide semiconductors (CMOS) will reach their functional limits within 10–15 years. Then, nanomaterials or molecular assemblies on the nanometer level will occupy the space. Promising concepts developed in recent years include single-electron devices that retain their scalability up to molecular level. Individual charge carriers can be handled by exploiting Coulombic effects in metallic single-electron devices with tunnel junctions with micrometer size. Such a field is termed single electronics (SE). The AuNPs have attracted the research's attention in the approach to bridge the gap between CMOS and true atomic scale in the future [26]. In the case of nanoelectronics, monodispersed nanoparticles have a potential lot. Metal nanoparticles having a diameter < 2 nm are required for such devices to achieve the Coulomb blockade effect at room temperature [27]. Researchers have synthesized AuNPs through a green synthetic procedure using *Solanum nigrum, Ricinus communis* and *Morus nigra*, etc., extract as reducing agents. They performed experiments to evaluate the effect of adding AuNPs in the DC electrical

conductivity and found that, with the increased addition of AuNPs, the DC electrical gradually increases [28]. Researchers have studied the size dependency of electronic properties of AuNPs nanoclusters up to 14 atoms through density functional theory and agree that the energetic and electronic properties of AuNPs nanoclusters depend on the size structures NPs [29].

2. Green Synthesis of Gold Nanoparticles (AuNPs) from Plants

Different physical and chemical synthesis protocols have been well known for the biosynthesis of AuNPs. However, most of those protocols were not well accepted due to toxic chemicals and elevated temperature in the synthesis process. They may be harmful to human beings and the environment [30][31]. The most common biosynthetic method is the extracellular nanoparticle production method [32]. The green synthesis of gold nanoparticles has been reported using plant tissues, bacteria, fungi, actinomycetes, etc. (**Figure 3**) [33]. However, the green synthesis of AuNPs from the plant is an eco-friendly approach. In the biosynthesis of AuNPs from the plant, different plant parts (leaf, bark, stem, root, etc.) are used as sources chopped into small pieces and boiled in distilled water to obtain the extract. By filtration and centrifugation, the extract can be purified. For metal salt solution $HAuCl_4$, $AgNO_3$ generally is mixed with plant extract at room temperature [34][33]. Plant extracts contain various metabolites or organic compounds (alkaloids, flavonoids, proteins, polysaccharides, cellulose, and phenolic compounds) and secondary metabolites, which are utilized for nanoparticle synthesis [35]. These can involve the bio reduction of metallic ions to NPs and act as stabilizing agents [36]. Plant extracts contain proteins that have functionalized amino groups ($–NH_2$) that can actively participate in the reduction reaction of AuNPs [29]. The functional groups (such as –C–O–C–, –C–O–, –C=C–, and –C=O–) present in phytochemicals, such as flavones, alkaloids, phenols, and anthracenes involve the generation of AuNPs. In this phenomenon, no external stabilising/capping agents are used because different phytochemicals act as reducing and stabilising/capping agents for the extracellular biosynthesis of AuNP, replacing the toxicity of chemicals such as sodium borohydride ($NaBH_4$) [37]. The bio reduction mechanism involves reducing metal ions from their mono or divalent oxidation state to a zero-valent state. After that, the nucleation of the reduced metal atoms takes place [38]. Ultimately, the metallic salt solution containing extract is reduced into Au^{3+} to Au^0, and the synthesis of AuNP proceeds within minutes to hours using a one-pot, single-step and eco-friendly method [39]. Due to the presence of a variety of phytochemicals in plant extract, no particular mechanism for this synthesis process is reported. The variation in composition and concentration of reducing agents in plant extracts is responsible for different sizes, shapes, and morphological nanoparticle synthesis [40]. Researchers have reported that the size and morphology of nanoparticles can be expected to be different by changing the synthesis parameters, including pH, metal salt, pH, temperature and reaction time [41].

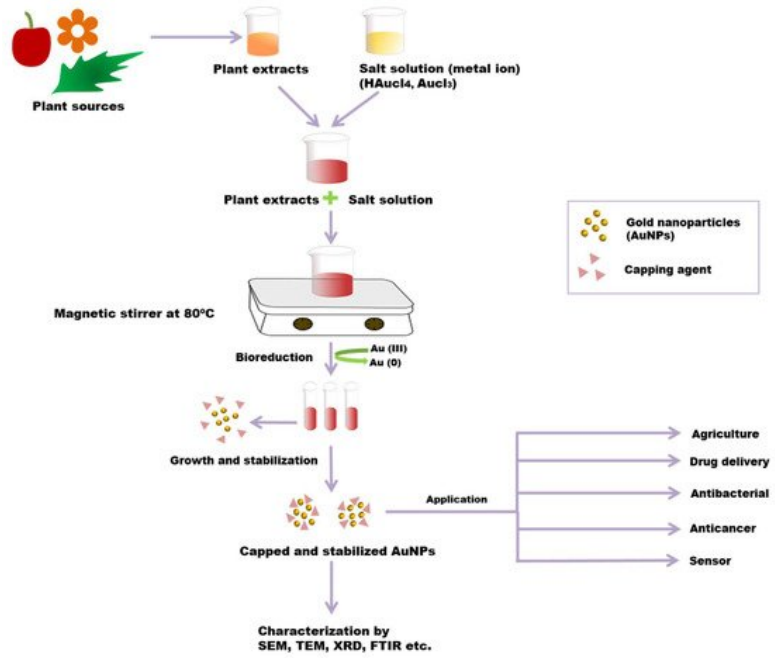

Figure 3. Green synthesis of AuNPs from a plant. Plant extract and metal salt solution $HAuCl_4$ were mixed. After that, the resultant solution is centrifuged, which results in the bio reduction of metallic ions to AuNPs. Phytochemicals act as reducing, as well as stabilizing/capping, agents in this process. The resultant AuNPs are characterized by using SEM, TEM, FTIR, XRD, etc.

Synthesized AuNPs were initially identified in the change in reaction colour (formation of red colour) through UV-vis spectrophotometer analysis. DLS, XRD and SAED confirmed the crystalline structure of gold nanoparticles, and the size, shape and distribution of nanoparticles were visualized by TEM image. Based on FTIR analysis, it can be confirmed that functional groups such as –C–O–C–, –C–O–, –C=C–, and –C=O are the capping ligands of the nanoparticles [42].

Different plant parts are used as a source for AuNP biosynthesis. Some green synthesized AuNPs from various plant parts are listed in **Table 2**.

Table 2. Green synthesis of Gold Nanoparticles (AuNPs) from different plants.

Plant	Plant Part	Reactive Compound	Salt Solution	Size (nm)	Shape	Characterization	Referenc
Artemisia vulgaris **(Mugwort)**	**Leaves**	**Polyphenols, flavonoids, terpenoids**	**$HAuCl_4$**	**50–100**	**Spherical, triangular, hexagonal**	**UV-vis Spectroscopy, XRD, FT-IR, DLS, ZP, TEM and EDX.**	[43]
Clitoria ternatea **(Asian pigeonwings)**	**Leaves**	**Alcoholic, amine groups, halo compounds**	**$HAuCl_4$**	**100**	**Rod**	**UV-vis spectroscopy, FTIR, XRD, TEM, EDX**	[44]
Murraya koenigii **Spreng (Curry leaves)**	**Leaves**	**Polyphenols, quercetin, quercetin-3-glucoside, flavonoids**	**$HAucl_4$**	**20–40**	**Spherical**	**XRD, EDX, FT-IR, HPLC, TEM, UV-vis spectra, Fluorescence microscopy.**	[45]
Artocarpus hirsutus **(Wild jack)**	**Leaves**	**Polyphenols, flavonoids, terpenoids**	**$HAuCl_4$**	**5–40**	**Spherical**	**XRD, UV-visible spectra, FT-IR and TEM**	[46]
Justicia glauca **(Thaasi murungai)**	**Leaves**	**Lignans[(+) pinoresinol, (+)-medioresinol], alkaloids, flavonoids, steroids (sitosterol-3-0-glucoside), terpenoids**	**$HAuCl{\cdot}3H_2O$**	**32**	**Hexagonl, spherical**	**UV-vis spectral analysis. X-ray, XRD, TEM, FTIR, EDX, CV, DPV.**	[47]
Terminalia arjuna **(Arjun tree)**	**Leaves**	**Arjunetin, leucoanthoc-yanidins, hydrolyzable tannins**	**$HAuCl_4$**	**20–25**	**Spherical**	**UV-visible spectra, FT-IR, XRD, AFM and TEM**	[48]
Memecylon umbellatum	**Leaves**	**Protein, saponins, polyphenols, carbohydrate**	**$HAuCl_4$, $AgNO_3$**	**15–25**	**Spherical, triangular, hexagonal**	**UV-visible spectra, FTIR, energy-dispersive x-ray spectroscopy, TEM,**	[49]
Mangifera indica	**Leaves**	**Terpenoids, flavonoids, thiamine**	**$HAuCl_4{\cdot}3H_2O$**	**17–20**	**Spherical**	**UV-vis, TEM and XRD.**	[50]
Olive	**Leaves**	**Proteins, oleoropein, apigenin-7-glucoside, luteolin-7-glucoside**	**$HAuCl_4{\cdot}3H_2O$**	**50–100**	**Triangular, spherical, hexagonal**	**UV-vis spectroscopy, photoluminescence, TEM, XRD, FTIR and thermogravimetric analysis.**	[51]
Coreopsis lanceolate	**Leaves**	**Antioxidants like sugars, flavonoids**	**$HAuCl_4$,**	**20–30**	**Spherical, quasi spherical**	**UV-vis spectroscopy, TEM and spectro fluorimetry**	[52]
Cassia auriculata **(Matura tea tree)**	**Leaves**	**Polysaccharides, flavonoids**	**$AuCl_3$, Au_2Cl_6**	**15–25**	**Spherical, triangular, hexagonal**	**X-ray diffraction, TEM, SEM-EDAX, FT-IR and visible absorption spectroscopy.**	[53]
Lonicera Japonica **(Japanese honeysuckle)**	**Flower**	**Amino acids**	**$AgNO_3$, $HAuCl_4$**	**8**	**Triangular tetrahedral**	**UV-vis spectrophotometer, FTIR, XRD, EDX, SEM and HRTEM.**	[54]
Nyctanthes arbortristis **(Night flowering jasmine)**	**Flower**	**alkaloids, flavonoids**	**$HAuCl_4$**	**15–25**	**Spherical**	**UV-vis spectro photometer, TEM, XRD, FTIR, NMR.**	[55]
Guazuma ulmifolia **(Bay cedar)**	**Bark**	**Tannins, proanthocya-nidins, precocene, catechins.**	**$HAuCl_4{\cdot}3H_2O$, $AgNO_3$**	**20–25**	**Spherical**	**UV-vis spectroscopy, FT-IR, XRD, AFM and HR-TEM analyses**	[56]

Plant	Plant Part	Reactive Compound	Salt Solution	Size (nm)	Shape	Characterization	Referenc
Salix (Willow tree)	Bark	Tannins, alkanoids, flavonoids, alkaloids.	$AuCl_4H_9O_4$	15	Spherical	UV-vis spectroscopy, XRD, TEM, and HR-TEM.	[57]
Acacia nilotica (Gum Arabic tree)	Bark	Protein, phenols, tannins, terpenoids, saponins	$HAuCl_4{\cdot}3H_2O$	10-15	Unshaped, quasispherical	UV-vis spectroscopy, XRD, EDX, TEM, FTIR, DPV.	[58]
Musa paradisiaca (Banana)	Peel	Phenolic compounds, gallocatechin, dopamine	$HAuCl_4$	50	Spherical	UV-vis spectroscopy, FTIR, XRD, TEM, Zeta potential analysis and EDX.	[59]
Mangifera indica Linn (Mango)	Peel	Phenols, carboxylic acids	$HAuCl_4$	3.26–21.68	Quasi-spherical	UV-vis spectrum, XRD, TEM, and FTIR.	[60]
Terminalia arjuna (Arjun tree)	Peel	Polyphenols	$HAuCl_4$	60	Triangular hexagonal pentagonl	UV spectroscopy, HRTEM, XRD, FESEM, EDX, DLS, and zeta potential analyses.	[61]
Lantana camara (Wild sage)	Fruit	Ursolic acid, iridoid glycosides, monoand sesquiterpe-nes, flavonoids	$HAuCl_4$	150–300	Triangular	UV-vis-NIR, TEM, SAED, DLS, and XRD techniques.	[62]
Citrus (Lemon, tangerine, orange)	Fruit	Citric acid, proteins	$HAuCl_4$	32.3, 43.4, 56.7	Spherical, triangular	UV-visible spectra. TEM XRD, SEAD, DLS.	[63]
Citrus maxima (Pomelo)	Fruit	Polypeptides/proteins, terpene, ascorbic acid	$HAuCl_4{\cdot}4H_2O$	15–35	Spherical	UV-vis spectroscopy, SEM, XRD and FTIR.	[64]
Pear	Fruit	Sugars, amino acids, proteins	$HAuCl_4$	20–400	Triangular hexagonalpolyhedral	UV-vis spectroscopy, TEM, AFM, XRD, XPS, EDAX.	[65]
Sterculia acuminate (Pola plant)	Fruit	Phenolic compounds	$HAuCl_4$	9.37–38.12	Spherical	TEM, X-ray diffraction, UV-vis spectroscopy and FTIR, and X-ray photoelectron spectrometry.	[66]
Pistacia integerrima (Zebra wood)	Galls	Monoterpenes, triterpenoids, sterols, dihydromal—valic acid.	$HAuCl_4{\cdot}3H_2O$	20–200	Grain-like	UV-vis spectroscopy, FTIR and SEM.	[67]
Abelmoschus esculentus (Okra)	Seed	Proteins, polysaccharides, glycoprotein	$HAuCl_4$	45–75	Spherical, uneven shape	UV-visible spectroscopy, XRD, FTIR, AFM, FESEM and EDX.	[68]
Theobromo cacao (Cocoa)	Seed	Polyphenols	$HAuCl_4$	150–200	Spherical	UV-vis-NIR spectrophotometer, SPR, TEM, XRD, FTIR, XPS	[69]
Hevea brasiliensis (Para rubber tree)	Latex	isoprene, proteins	$AuCl_3$, Au_2Cl_6	50	Spherical, triangular	UV-vis spectroscopy, SEM, TG/FT-IR, XED.	[70]
Zingiber officinale (Ginger)	Rhizome	Oxalic acid, ascorbic acid, Phenylpropanoids, zingerone.	$HAuCl_4$, $AgNO_3$	10–20	Spherical, triangular, truncated triangular, hexagonal	UV-visible spectroscopy, SEM-EDS, TEM, XRD, FTIR.	[71]
Curcuma longa (Turmeric)	Rhizome	Phenolic (curcumin), triterpenoids, alkaloid, sterols.	$HAuCl_4$, $AgNO_3$	5–60	Oblong spherical	UV-vis spectroscopy, XRD, TEM, HR-TEM, thermogravimetric analysis.	[72]

Plant	Plant Part	Reactive Compound	Salt Solution	Size (nm)	Shape	Characterization	Referenc
Panax ginseng C.A. Meyer (Korean red ginseng)	Rhizome	Saponin glycoside (ginsenoside), polysaccha-rides, flavones, peptide glycans	$HAuCl_4{\cdot}3H_2O$	2–40	Spherical	UV-visible spectra, TEM, FTIR.	[73]
Acorus calamus (Sweet flag)	Rhizome	Asarone, caryophyllene, isoasarone, methyl isoeugenol, safrole.	$HAuCl_4{\cdot}3H_2O$	10	Spherical	UV-visible spectral analysis, XRD and FT-IR, SPR, HR-TEM, SEM with EDAX.	[74][75]
Acacia nilotica (Gum Arabic tree)	Bark	Protein, phenols, tannins, terpenoids, Saponins.	$HAuCl_4{\cdot}3H_2O$	10–50	Unshaped, quasispherical.	UV-vis spectroscopy, XRD, TEM, EDX, DPV and FTIR.	[58]
Guazuma ulmifolia (Bay cedar)	Bark	Tannins, proanthocya-nidins, precocene, catechins.	$HAuCl_4{\cdot}3H_2O$ and $AgNO_3$	20–25	Spherical	UV-vis spectroscopy, FT-IR, XRD, AFM and HR-TEM analyses.	[56]
Areca catechu (Pinang palm)	Nut	Polyphenols, fats, proteins, carbohydrate, flavonoids.	$HAuCl_4$	13.70	Spherical	UV-visible, TEM, XRD, and FTIR.	[76]
Momordica Cochinchinensis.	Biomass	Proteins	$HAuCl_4$	10–80	Spherical, oval, triangular	UV-visible, FT-IR, XRD, TEM, SPR and EDX	[77]
Palm oil mill effluent	Palm oil	Proteins, flavonoids, reducing sugars, alkaloids	$HAuCl_4{\cdot}3H_2O$	13–25	Spherical	UV-vis spectroscopy, TEM, XRD, and FTIR.	[78]
Macrotylomauniflorum (Horse gram)	Whole plant	Proteins, carbohydrate, antioxidant	$HAuCl_4{\cdot}3H_2O$	14–17	Spherical	UV-visible spectroscopy, TEM, XRD and FTIR analysis.	[79]

2.1. Advantages and Limitations of the Synthesis Methods

Chemical methods for the synthesis of AuNPs have many limitations, which include environmental and biocompatibility concerns. Some of the chemicals used in the synthesis of gold nanoparticles during chemical synthesis can affect our environment and are the cause of risks for administering them into living organisms, thus limiting the biological applications of such AuNPs [80]. Therefore, various biological methods have been devised for the synthesis of AuNPs to limit these concerns. The green synthesis of AuNPs is a simple, safe, dynamic and facile process as its protocol follows a moderate environment without extreme temperatures or pressures. It is a cost-effective, rapid, environmentally benign, and biocompatible process, thus safe for clinical research. AuNPs are being synthesized through different physicochemical methods [81]. However, biogenic reduction of the gold salt to synthesize AuNPs is an inexpensive, eco-friendly and safe process. Neither toxic chemicals, such as sodium borohydride $NaBH_4$, are used, nor are any contaminants or harmful/dangerous by-products produced in this process. Moreover, a considerable number of AuNPs of controlled size and morphology can be easily synthesized. Their stability and reduction potential are attributed to bioactive molecules present in these biological resources. Green synthesized AuNPs application improves the diagnosis and treatment of many human diseases [37]. Out of many biological resources, plant extracts are reported to be a more beneficial resource. Various plant metabolites, such as alkaloids, polyphenols (catechin, flavones, taxifolin, catechin and epicatechin, and phenolic acids), alcoholic compounds, glutathiones, polysaccharides, antioxidants, organic acids (ascorbic, oxalic, malic, tartaric, and protocatechuic acid), quinones, proteins, and amino acids are involved in the formation of NPs by the reduction of metal ions. FT-IR and HPLC tests were used to indicate the presence of these capping agents in the synthesized NPs [35]. Therefore, in this prospect, using plant sources for Au NPs synthesis can open new horizons in future. The primary goal of green nanotechnology is to curtail forthcoming environmental and human health risks associated with the use of nanotechnology products and inspire the substitution of existing products with a more environmentally friendly nano-product. AuNPs synthesis through this green method can contribute to other fields such as green photocatalyst, drug delivery, anti-microorganism, adsorbent, detector, and green separation science and technology [36]. The green synthesis of AuNPs from bacteria is a slow process, so the synthesis process can take a long time, comprising hours and even days. Green synthesis from fungi is better than the previous one, as fungi produce a large number of proteins and reactive compounds. As a result, the reaction process can be scaled up using fungi as a source [75][82]. Although green synthesis of AuNPs from the plant has many advantages, the limitation of using a plant as a source for the synthesis of AuNPs is that the identification of reactive components is difficult as plant biomass comprises a

large number of organic components [83][84]. Biomolecules in the plant source contain various functional groups, which can play an essential role in synthesizing AuNPs, but different biomaterials show different reducing abilities. So, it is crucial to first determine their reducing ability before using them in the synthesis reaction [85][86].

2.2. Plant-Based Synthesized Gold Nanoparticles as Anticancer Agents

Increasing nanotechnology applications have gained broad attention in various sectors in recent years, but not restricted to medical, cosmetics, medical devices, electrical and electronic, drugs, food and packaging [87]. The most promising approach in nanotechnology is to develop nanomaterials for use in healthcare. In recent years, it has been observed that nanomaterials, such as gold nanoparticles (AuNPs), are of great interest to humans due to their wide range of uses in agriculture, remediation, medicine, health aspects, industry, pharmaceuticals, etc. [88]. Preliminary studies have shown that green synthesized AuNPs have various biological functions, such as antimicrobial, antiviral, anti-inflammatory, antioxidant and anticancer activity. In recent years, the use of plant-derived AuNPs has brought significant advances in cancer diagnosis and treatment, although some work in this area began mainly a few decades ago [87]. Notably, studies have demonstrated the usefulness of AuNPs as anticancer agents, in addition to photothermal agents, contrast agents and drug carriers. However, there are no previous literature reports on the molecular mechanism of tumour inhibition mediated by plant AuNPs. A recent resurgence of the anticancer effects of AuNPs from plant extracts has taken great strides so far. Despite these encouraging advances, more research is needed to understand the molecular consequences in cancer therapy, such as cellular toxicity, mitochondrial toxicity, apoptosis, necrosis and the production of reactive oxygen species (ROS). Several studies and reviews have been undertaken to investigate the anti-cancer potential of green synthesized AuNPs from different plant species. Scholars have reported on the green synthesis of AuNPs from several important plants and their applicability in various biomedical applications [89]; in this context, other authors have also proposed the implication of biosynthesized AuNPs in various applications. Researchers have reported on the aqueous and ethanolic extract of *Taxus baccata* synthesized nanostructure AuNPs. They were characterized by different techniques, such as UV–Vis spectroscopy, TEM, SEM and FT-IR. The MTT assay was performed to examine the anticancer activity of colloidal AuNPs on cell lines, such as Caov-4, MCF-7 and HeLa. In addition, an in vitro experiment on cell exposure to *T. baccata*-mediated AuNPs confirms the caspase-independent death program as an anti-cancer mechanism with increased efficacy for cancer therapy. This issue has been explored using flow-cytometry and real-time PCR [90]. Many plants (*Camellia sinensis*, *Coriandrum sativum*, *Mentha arvensis*, *Phyl-lanthus amarus*, *Artabotrys hexapetalus*, *Mimusops elengi*, *Syzygium aromaticum*) were described by Priya and Iyer, which showed that the green synthesized AuNPs have anticancer activity against the human breast cancer cell line, i.e., MCF7 and found that AuNPs at a minimum concentration of 2 µg/mL for cancer therapy are as effective as standard drugs. Moreover, the increase in the nanoparticle concentration is directly proportional to the effectiveness against cancer [91]. The increasing demand for biosynthesized gold nanoparticles has been greatly facilitated in medical applications, particularly in targeted drug delivery, one of the most recent advances in nanotechnology. Further studies have shown that the use of the *Dysosma pleiantha* rhizome can improve cancer therapy, which has been proven experimentally by tracking the biosynthesized AuNPs using an aqueous extract. The morphological characteristics of AuNPs are spherical with an average size of 127 nm, characterized by various techniques, such as UV-Vis spectroscopy, FT-IR, scanning electron microscopy (SEM) and transmission electron microscopy (TEM). In addition, they also suggested the promising role of biosynthesized AuNPs with enhanced activity against cell proliferation. Finally, they concluded that the *D. pleiantha* rhizome has antimetastatic potential by interfering with the microtubule polymerization in the human fibrosarcoma cell line HT-1080 [92]. It is clear from the previous research that green synthesized AuNPs holds better choice over other methods because of their cost-effectiveness, non-toxicity and feasibility in cancer therapy. However, this theory is backed up by the evidence in Virmani et al., from which the author concludes that biosynthesized nanoparticles have potential antitumor activity compared to chemically synthesized nanoparticles. They reviewed available methods that could be used to predict anticancer activity against many cancerous (HeLa, MCF-7, A549 and H1299) and normal (HEK293) cell lines. The extract derived from *Ocimum tenuiflorum* in the cell viability assay illustrates that biosynthesized AuNPs at lower concentrations were more pronounced and non-toxic, compared to HEK293, which can effectively inhibit the growth of various cancer cell lines with an IC_{50} value of 200 µg/mL. In contrast, the analysis shows that chemically synthesized nanoparticles have contributed negatively to anti-cancer properties even at high concentrations. The results conclude that the use of the chemically synthesized nanoparticles method for cancer therapy offers no obvious advantage [93]. Researchers have reported in their study that the internalization of AuNPs using the extract of *Allium cepa* was non-toxic to cells. *Allium cepa* has various pharmacological properties, including anti-cancer activity; however, over the past year, *Allium cepa*-derived nanoparticles have been of utmost importance in healthcare [94]. Moreover, some important applications of green synthesized AuNPs as an anti-cancer agent are summarized in **Table 1**. Mostly, the chemically synthesized gold nanoparticles (AuNPs) have been extensively exploited to date; only a few studies have been reported for plant-based green synthesized AuNP in vivo therapy, toxicity, and biodistribution. A study reported that green synthesized gold nanoparticles using leaf extract of *Peltophorum pterocarpum* (*PP*) for doxorubicin delivery both in vitro and in vivo in the C57BL6/J female mice. Administration of biosynthesized doxorubicin-loaded (b-Au-PP-Dox) drug delivery system displayed the significant inhibition of cancer cell growth (A549, B16F10) in vitro as well as inhibition of tumour growth in vivo model compared to free doxorubicin and untreated one [95]. Similarly, leaf extracts of *Mentha piperita*-generated AuNPs were tested against

MDA-MB-231 and A549, and normal 3T3-L1 cell lines in vitro, as well as the anti-inflammatory and analgesic activities, were studied on a Wistar rat model. AuNPs showed significant anticancer activities in vitro. However, the in vivo analysis gave positive results for both the activities with less potency as compared to the standard drugs, which suggests that AuNPs might be used in combination with standard drugs to enhance their efficacy [96]. These aforementioned novel in vivo studies have set a new frontier for the potential use of plant-based AuNPs for therapy and drug delivery systems as a cost-effective and eco-friendly approach in the near future. Multifunctionality is the key factor of nanovectors in cancer-specific therapy. Combinatorial therapy with phytoconstituents in cancer therapy has been thoroughly investigated and well documented in the present scenario. More recently, a re-evaluation of this concept has led to the use of a combination of phytochemicals which have been under constant investigation and are particularly used as potent natural anti-cancer agents. This was introduced to overcome some inherent limitations on toxicity, specificity, hazardous and reduced action. The anticancer activity on various cancer cell lines by AuNPs synthesized by using plant extracts are depicted in **Table 3**.

Table 3. Showing anticancer activity of gold nanoparticles using plant extracts and characterization technique.

Sl No.	Plant	Extract Used	Anticancer Activity Type	Characterization	Shape	Size	References
1	*Brazilian Red Propolis*	Hydroethanolic extract	Bladder (T24) and prostate (PC-3) cancer cell line	SPR, UV-Vis spectroscopy, NTA, TEM, EDXS, SAED, FTIR, TGA,	Spherical	8–15 nm	[97]
2	*Abies spectabilis*	Aqueous extract	Bladder cancer T24 cell line	TEM, SAED, UV-visible spectroscopy, EDX, FTIR, AFM, XRD	Spherical	20–200 nm	[98]
3	*Benincasa hispida*	Aqueous extract	HeLa cells and normal osteoblasts cell line	UV-Visible Spectroscopy, DLS, Zeta sizer, TEM, FTIR	Spherical	22.18 ± 2 nm	[99]
4	*Butea monosperma*	Aqueous water extract	Normal endothelial cells (HUVEC, ECV 304) and cancer cell lines (B16F10, MCF-7, HNGC2 and A549)	UV-visible spectroscopy, XRD, TEM, FTIR, DLS, XPS	Spherical, rod, triangular, hexagonal	30 nm	[100]
5	*orchid*	Orchid plant extract(whole)	Breast cancer AMJ 13 cell lines	UV-Vis spectroscopy, TEM, AFM, FTIR	Spherical	14–50 nm	[101]
6	*Taxus baccata*	Ethanolic extract	Breast (MCF7), cervical (HeLa), ovarian (Caov-4) cancer cell line	UV-Vis spectroscopy, TEM, Zetasizer, FTIR, EDX, AFM	Spherical, semispherical, hexagonal, triangular	20 nm	[90]
7	*Marsdenia tenacissima*	Leaf extract	A549 lung cell line	UV-vis, spectroscopy, AFM, EDS, TEM, FTIR, XRD, SAED	Spherical, anisotropic	50 nm	[102]
8	*Argemone mexicanaL.*	Aqueous extract	Human colon cancer cell line, HCT-15	TEM, XRD, FTIR	Hexagonal	20–40 nm	[103]
9	*Couroupita guianensis*	Aqueous extract	Leukemia cell line	UV-vis spectroscopy, FTIR, XRD, SEM, TEM	Spherical, triangular, tetragonal, pentagonal	7–48 nm	[104]
10	*Lycium chinense*	Fruit extract	Human breast cancer MCF7 cell line and non-diseased RAW264.7 (murine macrophage) cells	UV-vis spectroscopy, FTIR, XRD, FETEM, EDX, SAED	Poydispersed, agglomerated	20–100 nm	[105]
11	*Tabebuia argentiea*	Aqueous, flower extracts	Hepatic cells (Hep G2) cell line	EDX, SEM	Spherical	56 nm	[106]

Sl No.	Plant	Extract Used	Anticancer Activity Type	Characterization	Shape	Size	References
12	*Dendropanax morbifera*	Aqueous, leaf extract	A549 lung cancer cell line and human keratinocyte cell line	UV-Vis spectroscopy, EDX, FETEM, XRD, DLS	Polygonal, hexagonal	5–10 nm	[107]
13	*Halymenia dilatata*	Aqueous extract	Human colorectal adenocarcinoma cells (HT-29)	UV-Vis spectrophotometry, FTIR, XRD, FESEM, HRTEM, EDX, Zetasizer, DLS	Triangular, spherical	16 nm	[108]
14	*Dracocephalum kotschyi*	Leaf extract	Cervical cancer (HeLa), leukemia (K562) cell lines	UV-Vis spectrophotometry, TEM-SAED, SEM-EDAX, XRD, Zeta potential, DLS, FTIR	Spherical	11 nm	[109]
15	*Sargassum glaucescens*	Water extract (seaweed)	Cervical (HeLa), liver (HepG2), breast (MDA-MB-231), leukemia (CEM-ss) cell lines	UV-Vis spectroscopy, SEM, TEM, EDX	Spherical	3.65 ± 1.69 nm	[110]
16	*Trachyspermum ammi*	Seed extract	HepG2 cancer cell line	UV-Vis spectroscopy, XRD, TEM, DLS, FTIR	Spherical	16.63 nm	[111]
17	*Musa acuminata colla*	Aqueous, Flower extract	MCF-7, normal Vero cell line	UV-Vis, FTIR, XRD, SEM, EDAX	Spherical	10.1–15.6 nm	[112]
18	*aegle marmelos, eugenia jambolana and soursop*	Fruit extract	Human breast cancer cell line MCF-7	UV-Vis spectroscopy, TEM, FTIR, Zeta potentiometer	Spherical	18.28,16 nm	[113]
19	*Muntingia calabura*	Aqueous, fruit extract	Hep2 cells line	UV-Visible spectroscopy, DLS, FTIR, TEM	Spherical, oval	27 nm	[114]
20	*Nigella sativa*	Ethanolic leaf extract	Hep-G2 liver cancer cell line	TEM, XRD, EDS, FTIR, UV-Vis spectroscopy	Anisotropic	13–78 nm	[115]
21	*Marsilea quadrifolia L.*	Aqueous Leaf extract	PA-1 and A549 cell line	TEM, XRD, EDX, FTIR, UV-Vis spectroscopy	Spherical	10–40 nm	[116]
22	*Ocimum sanctum*	leaf extract	Dalton's lymphoma	UV-Vis spectroscopy, XRD, SEM, TEM, FTIR	Spherical	12–20 nm	[117]
23	*Bauhinia tomentosa Linn*	Aqueous, leaf extract	A549, HEp-2, MCF-7 cell line	FESEM, HRTEM, FTIR, EDX, XRD, TGA, UV-Vis spectroscopy	Spherical	11.5–40 nm	[118]
24	*Shorea tumbuggaia*	Bark extract	Thyroid cancer (SW579) cell lines	XRD, HRTEM, SAED, DLS, zeta potential, FTIR, UV-Vis spectroscopy	Spherical	20 nm	[119]
25	*walnut green*	Shell extract	MCF7 cells	UV-Vis spectroscopy, XRD, TEM,	Spherical, triangular	10–50 nm	[120]
26	*Cassia tora*	Leaf extract	Colon cancer cells	UV-Visible spectroscopy, FTIR, TEM, zeta potential, dark field microscopy	Spherical	57 nm	[121]

Sl No.	Plant	Extract Used	Anticancer Activity Type	Characterization	Shape	Size	References
27	*Abutilon indicum*	Water extract of leaves	HT-29 cells	UV-Vis spectroscopy, SPR, FTIR, DLS, EDAX, TEM, zeta potential, XRD, TGA	Spherical	1–20 nm	[122][123]
28	*Catharanthus roseus*	Water extract of Leaves	MCF7 and HepG2 cell line	UV-Vis spectroscopy, HRTEM, XRD, TEM	Spherical and triangular	15–28 nm	[122][124]
29	*Gymnema sylvestre*	Water extract of leaves	HT29 cell line	UV-Vis spectroscopy, SEM, EDAX, XRD, FTIR	Spherical	72.8 nm	[122][125]
30	*Hibiscus sabdariffa*	Water extract of leaves	U87 cell line	UV-vis spectroscopy, XRD, FTIR, XPS, TEM	Spherical	10–60 nm	[126][127]
31	*Hygrophila spinosa*	Water extract of leaf	HeLa cell line	XRD, SEM, EDAX, DLS, FTIR and UV-Vis spectroscopy.	Triangular and spherical	50–80 nm	[122][128]
32	*Moringa oleifera*	Water extract of leaves	A549 and SNO cells	DLS, TEM, UV-Vis spectroscopy, zeta potential	Spherical and polyhedral	10–20 nm	[122][129]
33	*Podophyllum hexandrum L.*	Water extract of leaves	HeLa cell line	UV-Vis spectroscopy, TEM, XRD, FTIR	Spherical	5–35 nm	[122][130]
34	*Elettaria cardamomum*	Seed, aqueous extract	HeLa cancer cell line	UV-Vis spectrophotometer, SAED, FTIR, XRD	Spherical	15.2 nm	[131]
35	*Coleous forskohlii*	Root extract	HEPG2 liver cancer cell line	UV-Vis spectrophotometer, HRTEM, FTIR, XRD, PSA	Spherical	10–30 nm	[132]
36	*Scutellaria barbata*	Aqueous extract	Pancreatic cancer cell lines (PANC-1)	UV-visible spectroscopy, TEM, SAED, AFM, FTIR, DLS, EDX	Spherical	0.4 µm–1 µm	[133]
37	*Sargassum incisifolium*	Aqueous extract	HT-29, MCF-7 cancer cell line, MCF-12a non cancer cell line	TEM, XRD, UV-Vis spectroscopy, zeta potential, FTIR, EDX, DLS, ICP-AES	Spherical	12.38 nm	[134]
38	*Panax notoginseng*	Leaf extract	PANC-1 cell line	UV-Vis spectroscopy, TEM, DLS, FTIR, AFM, SAED	Hexagonal, spherical, oval, triangular	80–12 nm	[133]
39	*Antigonon leptopus*	Leaf extract	Human adenocarcinoma breast cancer (MCF-7) cells	UV-Vis spectroscopy, XRD, SAED, FTIR, HRTEM, EDX	Spherical	13–28 nm	[135]
40	*Mukia Maderaspatna*	Aqueous, leaf extract	MCF 7 breast cancer cell line	UV-Vis spectroscopy, EDAX, SEM, TEM, FTIR	Spherical, circular, triangular	20–50 nm	[136]
41	*Hevea brasiliensis*	Latex extract	CHO-K1 cell line	UV-Vis spectroscopy, XRD, TEM, FTIR	spherical	9 nm	[137]
42	*Lonicera 4 japonica*	Flower extract	Cervical cancer (HeLa) cell line	UV-Vis spectroscopy, EDX, XRD, GCMS, TEM, FTIR	Polydisperse (spherical, triangular, hexagonal)	10–40 nm	[138]
43	*Anacardium occidentale*	Leaf extract	MCF-7 cell line	UV-Vis spectroscopy, TEM, XRD, FTIR	Spherical	10–30 nm	[139]

Sl No.	Plant	Extract Used	Anticancer Activity Type	Characterization	Shape	Size	References
44	*Sasa borealis*	Aqueous, leaf extract	AGS (Gastric adenocarcinoma) cell line	UV-Vis spectroscopy, TEM, EDX, XRD, FTIR, GCMS	Oval, spherical	10–30 nm	[140]
45	*Alternanthera Sessilis*	Aqueous, leaf extract	Cervical cancer (HeLa) cell line	UV-Vis spectroscopy, HRTEM, EDX, SAED, AFM, FTIR	Spherical	20–40 nm	[141]
46	*Bauhinia purpurea*	Aqueous, leaf extract	Lung carcinoma cell line (A549)	UV-Vis spectroscopy, HRTEM, SAED, XRD, EDX, FTIR	Spherical, polygonal	20–100 nm	[142]
47	*Crassocephalum rubens*	Aqueous, leaf extract	MCF-7 and Caco-2 cells	UV-Vis spectroscopy, TEM, FTIR	Spherical	20 ± 5 nm	[143]
48	*Backhousia citriodora*	Aqueous, leaf extract	MCF-7 breast cancer cell line and the HepG2 liver cancer cell line	UV-Vis spectroscopy, TEM, zeta potential, XRD, FTIR	Spherical	8.40 ± 0.084 nm	[144]
49	*Petroselinum crispum*	Aqueous, leaf extract	Human cancerous colorectal cell line	UV-Vis spectroscopy, TEM, EDX, FTIR.XRD	Spherical, semi-rod aggregates, flower-shaped nanoparticles	20–80 nm	[145]
50	*Indigofera tinctoria*	Aqueous, leaf extract	lung cancer cell line A549	UV-Vis. spectroscopy, FTIR, XRD, TEM, EDX, AFM	Spherical, triangular, hexagonal	6–29 nm	[146]

References

1. Sharma, N.; Bhatt, G.; Kothiyal, P. Gold Nanoparticles synthesis, properties, and forthcoming applications: A review. Ind ian J. Pharm. Biol. Res. 2015, 3, 13–27.
2. Jana, N.R.; Gearheart, L.; Murphy, C.J. Seeding Growth for Size Control of 5−40 nm Diameter Gold Nanoparticles. Lan gmuir 2001, 17, 6782–6786.
3. Brust, M.; Walker, M.; Bethell, D.; Schiffrin, D.J.; Whyman, R. Synthesis of thiol-derivatised gold nanoparticles in a two-phase Liquid–Liquid system. J. Chem. Soc. Chem. Commun. 1994, 801–802.
4. Turkevich, J.; Stevenson, P.C.; Hillier, J. A study of the nucleation and growth processes in the synthesis of colloidal gol d. Discuss. Faraday Soc. 1951, 11, 55–75.
5. Frens, G. Controlled Nucleation for the Regulation of the Particle Size in Monodisperse Gold Suspensions. Nat. Phys. Sci. 1973, 241, 20–22.
6. Zhao, L.; Jiang, D.; Cai, Y.; Ji, X.; Xie, R.; Yang, W. Tuning the size of gold nanoparticles in the citrate reduction by chlo ride ions. Nanoscale 2012, 4, 5071–5076.
7. Kim, J.H.; Kim, M.H.; Jo, D.H.; Yu, Y.S.; Lee, T.G.; Kim, J.H. The inhibition of retinal neovascularization by gold nanopar ticles via suppression of VEGFR-2 activation. Biomaterials 2011, 32, 1865–1871.
8. Zobel, M.; Neder, R.B.; Kimber, S.A. Universal solvent restructuring induced by colloidal nanoparticles. Science 2015, 3 47, 292–294.
9. Zheng, N.; Fan, J.; Stucky, G.D. One-Step One-Phase Synthesis of Monodisperse Noble-Metallic Nanoparticles and Th eir Colloidal Crystals. J. Am. Chem. Soc. 2006, 128, 6550–6551.
10. Song, J.; Kim, D.; Lee, D. Size Control in the Synthesis of 1–6 nm Gold Nanoparticles via Solvent-Controlled Nucleatio n. Langmuir 2011, 27, 13854–13860.
11. Stanglmair, C.; Scheeler, S.P.; Pacholski, C. Seeding Growth Approach to Gold Nanoparticles with Diameters Ranging f rom 10 to 80 Nanometers in Organic Solvent. Eur. J. Inorg. Chem. 2014, 2014, 3633–3637.
12. Ziegler, C.; Eychmüller, A. Seeded Growth Synthesis of Uniform Gold Nanoparticles with Diameters of 15−300 nm. J. P hys. Chem. C 2011, 115, 4502–4506.
13. Park, K.; Koerner, H.; Vaia, R.A. Depletion-Induced Shape and Size Selection of Gold Nanoparticles. Nano Lett. 2010, 10, 1433–1439.

14. Zhang, J.; Liu, H.; Wang, Z.; Ming, N. Shape-Selective Synthesis of Gold Nanoparticles with Controlled Sizes, Shapes, and Plasmon Resonances. Adv. Funct. Mater. 2007, 17, 3295–3303.
15. Wang, S.; Chen, K.-J.; Wu, T.-H.; Wang, H.; Lin, W.-Y.; Ohashi, M.; Chiou, P.-Y.; Tseng, H.-R. Photothermal effects of s upramolecularly assembled gold nanoparticles for the targeted treatment of cancer cells. Angew. Chem. Int. Ed. Engl. 2 010, 49, 3777–3781.
16. Wang, D.; Schaaf, P. Nanoporous gold nanoparticles. J. Mater. Chem. 2012, 22, 5344–5348.
17. Himmelhaus, M.; Takei, H. Cap-shaped gold nanoparticles for an optical biosensor. Sens. Actuators B Chem. 2000, 63, 24–30.
18. Robertson, J.D.; Rizzello, L.; Avila-Olias, M.; Gaitzsch, J.; Contini, C.; Magoń, M.S.; Renshaw, S.A.; Battaglia, G. Purifi cation of Nanoparticles by Size and Shape. Sci. Rep. 2016, 6, 27494.
19. Paino, I.M.M.; Marangoni, V.S.; de Oliveira, R.D.C.S.; Antunes, L.M.G.; Zucolotto, V. Cyto and genotoxicity of gold nan oparticles in human hepatocellular carcinoma and peripheral blood mononuclear cells. Toxicol. Lett. 2012, 215, 119–12 5.
20. Minati, L.; Benetti, F.; Chiappini, A.; Speranza, G. One-step synthesis of star-shaped gold nanoparticles. Colloids Surf. A Physicochem. Eng. Asp. 2014, 441, 623–628.
21. Amendola, V.; Pilot, R.; Frasconi, M.; Maragò, O.M.; Iatì, M.A. Surface plasmon resonance in gold nanoparticles: A revi ew. J. Phys. Condens. Matter 2017, 29, 203002.
22. Huang, X.; El-Sayed, M.A. Gold nanoparticles: Optical properties and implementations in cancer diagnosis and phototh ermal therapy. J. Adv. Res. 2010, 1, 13–28.
23. El-Brolossy, T.A.; Abdallah, T.; Mohamed, M.B.; Abdallah, S.; Easawi, K.; Negm, S.; Talaat, H. Shape and size depende nce of the surface plasmon resonance of gold nanoparticles studied by Photoacoustic technique. Eur. Phys. J. Spec. T op. 2008, 153, 361–364.
24. Nehl, C.L.; Hafner, J.H. Shape-dependent plasmon resonances of gold nanoparticles. J. Mater. Chem. 2008, 18, 2415–2419.
25. Rechberger, W.; Hohenau, A.; Leitner, A.; Krenn, J.R.; Lamprecht, B.; Aussenegg, F.R. Optical properties of two interact ing gold nanoparticles. Opt. Commun. 2003, 220, 137–141.
26. Schmid, G.; Simon, U. Gold nanoparticles: Assembly and electrical properties in 1–3 dimensions. Chem. Commun. 200 5, 697–710.
27. Teranishi, T. Fabrication and electronic properties of gold nanoparticle superlattices. Comptes Rendus Chim. 2003, 6, 9 79–987.
28. Asnag, G.M.; Oraby, A.H.; Abdelghany, A.M. Green synthesis of gold nanoparticles and its effect on the optical, thermal and electrical properties of carboxymethyl cellulose. Compos. Part. B Eng. 2019, 172, 436–446.
29. Li, S.; Shen, Y.; Xie, A.; Yu, X.; Qiu, L.; Zhang, L.; Zhang, Q. Green synthesis of silver nanoparticles using Capsicum an nuum L. extract. Green Chem. 2007, 9, 852–858.
30. Birla, S.S.; Tiwari, V.V.; Gade, A.K.; Ingle, A.P.; Yadav, A.P.; Rai, M.K. Fabrication of silver nanoparticles by Phoma glo merata and its combined effect against Escherichia coli, Pseudomonas aeruginosa and Staphylococcus aureus. Lett. A ppl. Microbiol. 2009, 48, 173–179.
31. Rai, M.; Yadav, A.; Gade, A. Current trends in phytosynthesis of metal nanoparticles. Crit. Rev. Biotechnol. 2008, 28, 27 7–284.
32. Lee, K.X.; Shameli, K.; Yew, Y.P.; Teow, S.-Y.; Jahangirian, H.; Rafiee-Moghaddam, R.; Webster, T.J. Recent Developm ents in the Facile Bio-Synthesis of Gold Nanoparticles (AuNPs) and Their Biomedical Applications. Int. J. Nanomed. 20 20, 15, 275–300.
33. Ahmed, S.; Annu; Ikram, S.; Yudha, S.S. Biosynthesis of gold nanoparticles: A green approach. J. Photochem. Photobi ol. B Biol. 2016, 161, 141–153.
34. Hassanisaadi, M.; Bonjar, G.H.; Rahdar, A.; Pandey, S.; Hosseinipour, A.; Abdolshahi, R. Environmentally Safe Biosynt hesis of Gold Nanoparticles Using Plant Water Extracts. Nanomaterials 2021, 11, 2033.
35. Marslin, G.; Siram, K.; Maqbool, Q.; Selvakesavan, R.K.; Kruszka, D.; Kachlicki, P.; Franklin, G. Secondary Metabolites in the Green Synthesis of Metallic Nanoparticles. Materials 2018, 11, 940.
36. Singh, J.; Dutta, T.; Kim, K.H.; Rawat, M.; Samddar, P.; Kumar, P. “Green” synthesis of metals and their oxide nanoparti cles: Applications for environmental remediation. J. Nanobiotechnology 2018, 16, 1–24.
37. Dauthal, P.; Mukhopadhyay, M. Noble Metal Nanoparticles: Plant-Mediated Synthesis, Mechanistic Aspects of Synthesi s, and Applications. Ind. Eng. Chem. Res. 2016, 55, 9557–9577.
38. Shah, M.; Fawcett, D.; Sharma, S.; Tripathy, S.K.; Poinern, G.E.J. Green Synthesis of Metallic Nanoparticles via Biologi cal Entities. Materials 2015, 8, 7278–7308.

39. Mittal, A.K.; Chisti, Y.; Banerjee, U.C. Synthesis of metallic nanoparticles using plant extracts. Biotechnol. Adv. 2013, 3 1, 346–356.

40. Kim, H.; Seo, Y.S.; Kim, K.; Han, J.W.; Park, Y.; Cho, S. Concentration Effect of Reducing Agents on Green Synthesis o f Gold Nanoparticles: Size, Morphology, and Growth Mechanism. Nanoscale Res. Lett. 2016, 11, 230.

41. Zhang, D.; Ma, X.; Gu, Y.; Huang, H.; Zhang, G. Green Synthesis of Metallic Nanoparticles and Their Potential Applicati ons to Treat Cancer. Front. Chem. 2020, 8, 799.

42. Mude, N.; Ingle, A.; Gade, A.; Rai, M. Synthesis of Silver Nanoparticles Using Callus Extract of Carica papaya—A First Report. J. Plant. Biochem. Biotechnol. 2009, 18, 83–86.

43. Sundararajan, B.; Ranjitha Kumari, B.D. Novel synthesis of gold nanoparticles using Artemisia vulgaris L. leaf extract a nd their efficacy of larvicidal activity against dengue fever vector Aedes aegypti L. J. Trace Elem. Med. Biol. Organ Soc. Miner. Trace Elem. 2017, 43, 187–196.

44. Vanaraj, S.; Jabastin, J.; Sathiskumar, S.; Preethi, K. Production and Characterization of Bio-AuNPs to Induce Synergis tic Effect Against Multidrug Resistant Bacterial Biofilm. J. Clust. Sci. 2017, 28, 227–244.

45. Alam, M.N.; Das, S.; Batuta, S.; Roy, N.; Chatterjee, A.; Mandal, D.; Begum, N.A. Murraya koenegii Spreng. Leaf Extra ct: An Efficient Green Multifunctional Agent for the Controlled Synthesis of Au Nanoparticles. ACS Sustain. Chem. Eng. 2014, 2, 652–664.

46. Vijayashree, I.S.; Niranjana, P.; Prabhu, G.; Sureshbabu, V.V.; Manjanna, J. Conjugation of Au Nanoparticles with Chlor ambucil for Improved Anticancer Activity. J. Clust. Sci. 2017, 28, 133–148.

47. Karuppiah, C.; Palanisamy, S.; Chen, S.-M.; Emmanuel, R.; Muthupandi, K.; Prakash, P. Green synthesis of gold nano particles and its application for the trace level determination of painter's colic. RSC Adv. 2015, 5, 16284–16291.

48. Gopinath, K.; Venkatesh, K.S.; Ilangovan, R.; Sankaranarayanan, K.; Arumugam, A. Green synthesis of gold nanoparti cles from leaf extract of Terminalia arjuna, for the enhanced mitotic cell division and pollen germination activity. Ind. Cro ps Prod. 2013, 50, 737–742.

49. Arunachalam, K.D.; Annamalai, S.K.; Hari, S. One-step green synthesis and characterization of leaf extract-mediated bi ocompatible silver and gold nanoparticles from Memecylon umbellatum. Int. J. Nanomed. 2013, 8, 1307–1315.

50. Philip, D. Rapid green synthesis of spherical gold nanoparticles using Mangifera indica leaf. Spectrochim. Acta Part. A Mol. Biomol. Spectrosc. 2010, 77, 807–810.

51. Khalil, M.M.H.; Ismail, E.H.; El-Magdoub, F. Biosynthesis of Au nanoparticles using olive leaf extract: 1st Nano Update s. Arab. J. Chem. 2012, 5, 431–437.

52. Abhijith, K.S.; Thakur, M.S. Application of green synthesis of gold nanoparticles for sensitive detection of aflatoxin B1 b ased on metal enhanced fluorescence. Anal. Methods 2012, 4, 4250–4256.

53. Kumar, V.G.; Gokavarapu, S.D.; Rajeswari, A.; Dhas, T.S.; Karthick, V.; Kapadia, Z.; Shrestha, T.; Barathy, I.A.; Roy, A.; Sinha, S. Facile green synthesis of gold nanoparticles using leaf extract of antidiabetic potent Cassia auriculata. Colloid s Surf. B. Biointerfaces 2011, 87, 159–163.

54. Nagajyothi, P.C.; Lee, S.E.; An, M.; Lee, K.D. Green synthesis of silver and gold nanoparticles using Lonicera Japonica flower extract. Bull. Korean Chem. Soc. 2012, 33, 2609–2612.

55. Das, R.K.; Gogoi, N.; Bora, U. Green synthesis of gold nanoparticles using Nyctanthes arbortristis flower extract. Biopr ocess. Biosyst. Eng. 2011, 34, 615–619.

56. Karthika, V.; Arumugam, A.; Gopinath, K.; Kaleeswarran, P.; Govindarajan, M.; Alharbi, N.S.; Kadaikunnan, S.; Khaled, J.M.; Benelli, G. Guazuma ulmifolia bark-synthesized Ag, Au and Ag/Au alloy nanoparticles: Photocatalytic potential, D NA/protein interactions, anticancer activity and toxicity against 14 species of microbial pathogens. J. Photochem. Photo biol. B 2017, 167, 189–199.

57. Bahram, M.; Mohammadzadeh, E. Green synthesis of gold nanoparticles with willow tree bark extract: A sensitive colou rimetric sensor for cysteine detection. Anal. Methods 2014, 6, 6916–6924.

58. Emmanuel, R.; Karuppiah, C.; Chen, S.-M.; Palanisamy, S.; Padmavathy, S.; Prakash, P. Green synthesis of gold nano particles for trace level detection of a hazardous pollutant (nitrobenzene) causing Methemoglobinaemia. J. Hazard. Mat er. 2014, 279, 117–124.

59. Vijayakumar, S.; Vaseeharan, B.; Malaikozhundan, B.; Gopi, N.; Ekambaram, P.; Pachaiappan, R.; Velusamy, P.; Murug an, K.; Benelli, G.; Suresh Kumar, R.; et al. Therapeutic effects of gold nanoparticles synthesized using Musa paradisia ca peel extract against multiple antibiotic resistant Enterococcus faecalis biofilms and human lung cancer cells (A549). Microb. Pathog. 2017, 102, 173–183.

60. Yang, N.; WeiHong, L.; Hao, L. Biosynthesis of Au nanoparticles using agricultural waste mango peel extract and its in vitro cytotoxic effect on two normal cells. Mater. Lett. 2014, 134, 67–70.

61. Suganthy, N.; Sri Ramkumar, V.; Pugazhendhi, A.; Benelli, G.; Archunan, G. Biogenic synthesis of gold nanoparticles fr om Terminalia arjuna bark extract: Assessment of safety aspects and neuroprotective potential via antioxidant, anticholi

nesterase, and antiamyloidogenic effects. Environ. Sci. Pollut. Res. Int. 2018, 25, 10418–10433.

62. Kumar, B.; Smita, K.; Cumbal, L.; Debut, A. Extracellular biofabrication of gold nanoparticles by using Lantana camara berry extract. Inorg. Nano-Metal. Chem. 2017, 47, 138–142.

63. Sujitha, M.V.; Kannan, S. Green synthesis of gold nanoparticles using Citrus fruits (Citrus limon, Citrus reticulata and Ci trus sinensis) aqueous extract and its characterization. Spectrochim. Acta. A Mol. Biomol. Spectrosc. 2013, 102, 15–23.

64. Yu, J.; Xu, D.; Guan, H.N.; Wang, C.; Huang, L.K.; Chi, D.F. Facile one-step green synthesis of gold nanoparticles usin g Citrus maxima aqueous extracts and its catalytic activity. Mater. Lett. 2016, 166, 110–112.

65. Ghodake, G.; Lee, D. Green synthesis of gold nanostructures using pear extract as effective reducing and coordinating agent. Korean J. Chem. Eng. 2011, 28, 2329–2335.

66. Rodríguez-León, E.; Rodríguez-Vázquez, B.E.; Martínez-Higuera, A.; Rodríguez-Beas, C.; Larios-Rodríguez, E.; Navar ro, R.E.; López-Esparza, R.; Iñiguez-Palomares, R.A. Synthesis of Gold Nanoparticles Using Mimosa tenuiflora Extrac t, Assessments of Cytotoxicity, Cellular Uptake, and Catalysis. Nanoscale Res. Lett. 2019, 14, 334.

67. Islam, N.U.; Jalil, K.; Shahid, M.; Muhammad, N.; Rauf, A. Pistacia integerrima gall extract mediated green synthesis of gold nanoparticles and their biological activities. Arab. J. Chem. 2019, 12, 2310–2319.

68. Jayaseelan, C.; Ramkumar, R.; Rahuman, A.A.; Perumal, P. Green synthesis of gold nanoparticles using seed aqueous extract of Abelmoschus esculentus and its antifungal activity. Ind. Crops Prod. 2013, 45, 423–429.

69. Fazal, S.; Jayasree, A.; Sasidharan, S.; Koyakutty, M.; Nair, S.V.; Menon, D. Green Synthesis of Anisotropic Gold Nano particles for Photothermal Therapy of Cancer. ACS Appl. Mater. Interfaces 2014, 6, 8080–8089.

70. Cabrera, F.C.; Mohan, H.; dos Santos, R.J.; Agostini, D.L.S.; Aroca, R.F.; Rodríguez-Pérez, M.A.; Job, A.E. Green Synt hesis of Gold Nanoparticles with Self-Sustained Natural Rubber Membranes. J. Nanomater. 2013, 2013, 710902.

71. Velmurugan, P.; Anbalagan, K.; Manosathyadevan, M.; Lee, K.-J.; Cho, M.; Lee, S.-M.; Park, J.-H.; Oh, S.-G.; Bang, K.- S.; Oh, B.-T. Green synthesis of silver and gold nanoparticles using Zingiber officinale root extract and antibacterial acti vity of silver nanoparticles against food pathogens. Bioprocess. Biosyst. Eng. 2014, 37, 1935–1943.

72. Nadagouda, M.N.; Iyanna, N.; Lalley, J.; Han, C.; Dionysiou, D.D.; Varma, R.S. Synthesis of Silver and Gold Nanopartic les Using Antioxidants from Blackberry, Blueberry, Pomegranate, and Turmeric Extracts. ACS Sustain. Chem. Eng. 201 4, 2, 1717–1723.

73. Leonard, K.; Ahmmad, B.; Okamura, H.; Kurawaki, J. In situ green synthesis of biocompatible ginseng capped gold nan oparticles with remarkable stability. Colloids Surf. B. Biointerfaces 2011, 82, 391–396.

74. Ganesan, R.M.; Gurumallesh Prabu, H. Synthesis of gold nanoparticles using herbal Acorus calamus rhizome extract a nd coating on cotton fabric for antibacterial and UV blocking applications. Arab. J. Chem. 2019, 12, 2166–2174.

75. Sathiyanarayanan, G.; Vignesh, V.; Saibaba, G.; Vinothkanna, A.; Dineshkumar, K.; Viswanathan, M.B.; Selvin, J. Synt hesis of carbohydrate polymer encrusted gold nanoparticles using bacterial exopolysaccharide: A novel and greener ap proach. RSC Adv. 2014, 4, 22817–22827.

76. Rajan, A.; Vilas, V.; Philip, D. Studies on catalytic, antioxidant, antibacterial and anticancer activities of biogenic gold na noparticles. J. Mol. Liq. 2015, 212, 331–339.

77. Paul, B.; Bhuyan, B.; Purkayastha, D.D.; Vadivel, S.; Dhar, S.S. One-pot green synthesis of gold nanoparticles and stu dies of their anticoagulative and photocatalytic activities. Mater. Lett. 2016, 185, 143–147.

78. Gan, P.P.; Ng, S.H.; Huang, Y.; Li, S.F.Y. Green synthesis of gold nanoparticles using palm oil mill effluent (POME): A lo w-cost and eco-friendly viable approach. Bioresour. Technol. 2012, 113, 132–135.

79. Aromal, S.A.; Vidhu, V.K.; Philip, D. Green synthesis of well-dispersed gold nanoparticles using Macrotyloma uniflorum. Spectrochim. Acta Part. A Mol. Biomol. Spectrosc. 2012, 85, 99–104.

80. Chen, Y.-S.; Hung, Y.-C.; Liau, I.; Huang, G.S. Assessment of the In Vivo Toxicity of Gold Nanoparticles. Nanoscale Re s. Lett. 2009, 4, 858–864.

81. Kumar, B. Green Synthesis of Gold, Silver, and Iron Nanoparticles for the Degradation of Organic Pollutants in Wastew ater. J. Compos. Sci. 2021, 5, 219.

82. Ganaie, S.U.; Abbasi, T.; Anuradha, J.; Abbasi, S.A. Biomimetic synthesis of silver nanoparticles using the amphibious weed ipomoea and their application in pollution control. J. King Saud Univ.-Sci. 2014, 26, 222–229.

83. Teimuri-mofrad, R.; Hadi, R.; Tahmasebi, B.; Farhoudian, S.; Mehravar, M.; Nasiri, R. Green synthesis of gold nanoparti cles using plant extract: Mini-review. Nanochemistry Res. 2017, 2, 8–19.

84. Siddiqi, K.S.; Husen, A. Recent advances in plant-mediated engineered gold nanoparticles and their application in biolo gical system. J. Trace Elem. Med. Biol. Organ Soc. Miner. Trace Elem. 2017, 40, 10–23.

85. Chen, Y.; Wu, X.; Lv, L.; Li, F.; Liu, Z.; Kong, Q.; Li, C. Enhancing reducing ability of α-zein by fibrillation for synthesis of Au nanocrystals with continuous flow catalysis. J. Colloid Interface Sci. 2017, 491, 37–43.

86. Lee, J.; Kim, H.Y.; Zhou, H.; Hwang, S.; Koh, K.; Han, D.-W.; Lee, J. Green synthesis of phytochemical-stabilized Au na noparticles under ambient conditions and their biocompatibility and antioxidative activity. J. Mater. Chem. 2011, 21, 133 16–13326.
87. Cai, W.; Gao, T.; Hong, H. Applications of gold nanoparticles in cancer nanotechnology. Nanotechnol. Sci. Appl. 2008, 1, 17.
88. Mu, L.; Sprando, R.L. Application of Nanotechnology in Cosmetics. Pharm. Res. 2010, 27, 1746–1749.
89. Khan, T.; Ullah, N.; Khan, M.A.; Mashwani, Z.-R.; Nadhman, A. Plant-based gold nanoparticles; a comprehensive revie w of the decade-long research on synthesis, mechanistic aspects and diverse applications. Adv. Colloid Interface Sci. 2 019, 272, 102017.
90. Kajani, A.A.; Bordbar, A.-K.; Zarkesh Esfahani, S.H.; Razmjou, A. Gold nanoparticles as potent anticancer agent: Green synthesis, characterization, and in vitro study. RSC Adv. 2016, 6, 63973–63983.
91. MR Kamala Priya, P.I. Anticancer studies of the synthesized gold nanoparticles against MCF 7 breast cancer cell lines. Appl. Nanosci. 2015, 5, 443.
92. Karuppaiya, P.; Satheeshkumar, E.; Chao, W.T.; Kao, L.Y.; Chen, E.C.F.; Tsay, H.S. Anti-metastatic activity of biologicall y synthesized gold nanoparticles on human fibrosarcoma cell line HT-1080. Colloids Surf. B Biointerfaces 2013, 110, 1 63–170.
93. Virmani, I.; Sasi, C.; Priyadarshini, E.; Kumar, R.; Sharma, S.K.; Singh, G.P.; Pachwarya, R.B.; Paulraj, R.; Barabadi, H.; Saravanan, M.; et al. Comparative Anticancer Potential of Biologically and Chemically Synthesized Gold Nanopartic les. J. Clust. Sci. 2020, 31, 867–876.
94. UK Parida, B.B.P.N. Green synthesis and characterization of gold nanoparticles using onion (Allium cepa) extract. Worl d J. Nano Sci. Eng. 2011, 1, 93–98.
95. Mukherjee, S.; Sau, S.C.; Madhuri, D.; Bollu, V.S.; Madhusudana, K.; Sreedhar, B.; Banerjee, R.; Patra, C.R. Green Sy nthesis and Characterization of Monodispersed Gold Nanoparticles: Toxicity Study, Delivery of Doxorubicin and Its Bio-Distribution in Mouse Model. J. Biomed. Nanotechnol. 2016, 121, 165–181.
96. Ahmad, N.; Bhatnagar, S.; Saxena, R.; Iqbal, D.; Ghosh, A.K.; Dutta, R. Biosynthesis and characterization of gold nano particles: Kinetics, in vitro and in vivo study. Mater. Sci. Eng. C Mater. Biol. Appl. 2017, 78, 553–564.
97. Botteon, C.E.A.; Silva, L.B.; Ccana-Ccapatinta, G.V.; Silva, T.S.; Ambrosio, S.R.; Veneziani, R.C.S.; Bastos, J.K.; Marc ato, P.D. Biosynthesis and characterization of gold nanoparticles using Brazilian red propolis and evaluation of its antim icrobial and anticancer activities. Sci. Rep. 2021, 11, 1974.
98. Wu, T.; Duan, X.; Hu, C.; Wu, C.; Chen, X.; Huang, J.; Liu, J.; Cui, S. Synthesis and characterization of gold nanoparticl es from Abies spectabilis extract and its anticancer activity on bladder cancer T24 cells. Artif. Cells Nanomed. Biotechn ol. 2019, 47, 512–523.
99. Al Saqr, A.; Khafagy, E.-S.; Alalaiwe, A.; Aldawsari, M.F.; Alshahrani, S.M.; Anwer, M.K.; Khan, S.; Lila, A.S.A.; Arab, H. H.; Hegazy, W.A.H. Synthesis of Gold Nanoparticles by Using Green Machinery: Characterization and In Vitro Toxicity. Nanomaterials 2021, 11, 808.
100. Patra, S.; Mukherjee, S.; Barui, A.K.; Ganguly, A.; Sreedhar, B.; Patra, C.R. Green synthesis, characterization of gold a nd silver nanoparticles and their potential application for cancer therapeutics. Mater. Sci. Eng. C Mater. Biol. Appl. 201 5, 53, 298–309.
101. Yas, R.M.; Ghafoor, D.A.; Saeed, M.A. Anticancer effect of green synthesized gold nanoparticles using orchid extract a nd their characterizations on breast cancer AMJ-13 Cell line. Syst. Rev. Pharm. 2021, 12, 500–505.
102. Sun, B.; Hu, N.; Han, L.; Pi, Y.; Gao, Y.; Chen, K. Anticancer activity of green synthesised gold nanoparticles from Mars denia tenacissima inhibits A549 cell proliferation through the apoptotic pathway. Artif. Cells Nanomed. Biotechnol. 201 9, 47, 4012–4019.
103. Datkhile, K.D.; Patil, S.R.; Durgawale, P.P.; Patil, M.N.; Hinge, D.D.; Jagdale, N.J.; Deshmukh, V.N.; More, A.L. Biogeni c synthesis of gold nanoparticles using Argemone mexicana L. and their cytotoxic and genotoxic effects on human colo n cancer cell line (HCT-15). J. Genet. Eng. Biotechnol. 2021, 19, 9.
104. Geetha, R.; Ashokkumar, T.; Tamilselvan, S.; Govindaraju, K.; Sadiq, M.; Singaravelu, G. Green synthesis of gold nano particles and their anticancer activity. Cancer Nanotechnol. 2013, 4, 91–98.
105. Chokkalingam, M.; Singh, P.; Huo, Y.; Soshnikova, V.; Ahn, S.; Kang, J.; Mathiyalagan, R.; Kim, Y.J.; Yang, D.C. Facile synthesis of Au and Ag nanoparticles using fruit extract of Lycium chinense and their anticancer activity. J. Drug Deliv. Sci. Technol. 2019, 49, 308–315.
106. Reddy, M. Synthesis of gold nanoparticles from the flower extracts of tabebuia argentiea and their anticancer activity. In t. J. Pharm. Biol. Sci. 2017, 8, 379–383.
107. Wang, C.; Mathiyalagan, R.; Kim, Y.J.; Castro-Aceituno, V.; Singh, P.; Ahn, S.; Wang, D.; Yang, D.C. Rapid green synth esis of silver and gold nanoparticles using Dendropanax morbifera leaf extract and their anticancer activities. Int. J. Nan

omed. 2016, 11, 3691–3701.

108. Vinosha, M.; Palanisamy, S.; Muthukrishnan, R.; Selvam, S.; Kannapiran, E.; You, S.; Prabhu, N.M. Biogenic synthesis of gold nanoparticles from Halymenia dilatata for pharmaceutical applications: Antioxidant, anti-cancer and antibacterial activities. Process. Biochem. 2019, 85, 219–229.

109. Dorosti, N.; Jamshidi, F. Plant-mediated gold nanoparticles by Dracocephalum kotschyi as anticholinesterase agent: Sy nthesis, characterization, and evaluation of anticancer and antibacterial activity. J. Appl. Biomed. 2016, 14, 235–245.

110. Ajdari, Z.; Rahman, H.; Shameli, K.; Abdullah, R.; Abd Ghani, M.; Yeap, S.; Abbasiliasi, S.; Ajdari, D.; Ariff, A. Novel Gol d Nanoparticles Reduced by Sargassum glaucescens: Preparation, Characterization and Anticancer Activity. Molecules 2016, 21, 123.

111. Perveen, K.; Husain, F.M.; Qais, F.A.; Khan, A.; Razak, S.; Afsar, T.; Alam, P.; Almajwal, A.M.; Abulmeaty, M.M.A. Micro wave-Assisted Rapid Green Synthesis of Gold Nanoparticles Using Seed Extract of Trachyspermum ammi: ROS Media ted Biofilm Inhibition and Anticancer Activity. Biomolecules 2021, 11, 197.

112. Valsalam, S.; Agastian, P.; Esmail, G.A.; Ghilan, A.-K.M.; Al-Dhabi, N.A.; Arasu, M.V. Biosynthesis of silver and gold na noparticles using Musa acuminata colla flower and its pharmaceutical activity against bacteria and anticancer efficacy. J. Photochem. Photobiol. B Biol. 2019, 201, 111670.

113. Vijayakumar, S. Eco-friendly synthesis of gold nanoparticles using fruit extracts and in vitro anticancer studies. J. Saudi Chem. Soc. 2019, 23, 753–761.

114. Kumar, P.S.; Jeyalatha, M.V.; Malathi, J.; Ignacimuthu, S. Anticancer effects of one-pot synthesized biogenic gold nano particles (Mc-AuNps) against laryngeal carcinoma. J. Drug Deliv. Sci. Technol. 2018, 44, 118–128.

115. Gothainayagi, A.; Josephine, N.M. Characterization of green synthesized gold nanoparticles from Nigella sativa oil and evaluation of its antibacterial and anticancer activity. J. Crit. Rev. 2020, 7, 1664–1679.

116. Balashanmugam, P.; Mosachristas, K.; Kowsalya, E. In vitro cytotoxicity and antioxidant evaluation of biogenic synthesi zed gold nanoparticles from Marsilea quadrifolia on lung and ovarian cancer cells. Int. J. Appl. Pharm. 2018, 10, 153–1 58.

117. Gautam, P.K.; Kumar, S.; Tomar, M.S.; Singh, R.K.; Acharya, A. Biologically Synthesized Gold Nanoparticles using Oci mum sanctum (Tulsi Leaf Extract) Induced Anti-Tumor Response in a T Cell Daltons Lymphoma. J. Cell Sci. Ther. 201 7, 8, 2.

118. Mukundan, D.; Mohankumar, R.; Vasanthakumari, R. Comparative study of synthesized silver and gold nanoparticles u sing leaves extract of Bauhinia tomentosa Linn and their anticancer efficacy. Bull. Mater. Sci. 2017, 40, 335–344.

119. Li, Y.M.; Wang, Y.Y.; Cheng, B.N. In-vitro cytotoxicity of biosynthesized gold nanoparticles against thyroid cancer cell lin es. Trop. J. Pharm. Res. 2017, 16, 1523–1528.

120. Rabori, M.S.; Karimabad, M.N.; Hajizadeh, M.R. Facile, low-cost and rapid phytosynthesis of stable and eco-friendly go ld nanoparticles using green walnut shell and study of their anticancer potential. World Cancer Res. J. 2021, 8, 1–8.

121. Abel, E.E.; John Poonga, P.R.; Panicker, S.G. Characterization and in vitro studies on anticancer, antioxidant activity ag ainst colon cancer cell line of gold nanoparticles capped with Cassia tora SM leaf extract. Appl. Nanosci. 2016, 6, 121–129.

122. Patil, M.P.; Ngabire, D.; Thi, H.H.P.; Kim, M.-D.; Kim, G.-D. Eco-friendly Synthesis of Gold Nanoparticles and Evaluatio n of Their Cytotoxic Activity on Cancer Cells. J. Clust. Sci. 2017, 28, 119–132.

123. Mata, R.; Nakkala, J.R.; Sadras, S.R. Polyphenol stabilized colloidal gold nanoparticles from Abutilon indicum leaf extra ct induce apoptosis in HT-29 colon cancer cells. Colloids Surf. B. Biointerfaces 2016, 143, 499–510.

124. Muthukumar, T.; Sudhakumari; Sambandam, B.; Aravinthan, A.; Sastry, T.P.; Kim, J.-H. Green synthesis of gold nanopa rticles and their enhanced synergistic antitumor activity using HepG2 and MCF7 cells and its antibacterial effects. Proc ess. Biochem. 2016, 51, 384–391.

125. Arunachalam, K.D.; Arun, L.B.; Annamalai, S.K.; Arunachalam, A.M. Biofunctionalized gold nanoparticles synthesis fro m Gymnema sylvestre and its preliminary anticancer activity. Int. J. Pharm. Pharm. Sci. 2014, 6, 423–430.

126. Mishra, P.; Ray, S.; Sinha, S.; Das, B.; Khan, M.I.; Behera, S.K.; Yun, S.-I.; Tripathy, S.K.; Mishra, A. Facile bio-synthesi s of gold nanoparticles by using extract of Hibiscus sabdariffa and evaluation of its cytotoxicity against U87 glioblastom a cells under hyperglycemic condition. Biochem. Eng. J. 2016, 105, 264–272.

127. Patil, M.P.; Kim, G.-D. Eco-friendly approach for nanoparticles synthesis and mechanism behind antibacterial activity of silver and anticancer activity of gold nanoparticles. Appl. Microbiol. Biotechnol. 2017, 101, 79–92.

128. Koperuncholan, M. Bioreduction of chloroauric acid (HAuCl4) for the synthesis of gold nanoparticles (GNPs): A special empathies of pharmacological activity. Int. J. Phytopharm. 2015, 5, 72–80.

129. Tiloke, C.; Phulukdaree, A.; Anand, K.; Gengan, R.M.; Chuturgoon, A.A. Moringa oleifera Gold Nanoparticles Modulate Oncogenes, Tumor Suppressor Genes, and Caspase-9 Splice Variants in A549 Cells. J. Cell. Biochem. 2016, 117, 230 2–2314.

130. Jeyaraj, M.; Arun, R.; Sathishkumar, G.; MubarakAli, D.; Rajesh, M.; Sivanandhan, G.; Kapildev, G.; Manickavasagam, M.; Thajuddin, N.; Ganapathi, A. An evidence on G2/M arrest, DNA damage and caspase mediated apoptotic effect of b iosynthesized gold nanoparticles on human cervical carcinoma cells (HeLa). Mater. Res. Bull. 2014, 52, 15–24.
131. Rajan, A.; Rajan, A.R.; Philip, D. Elettaria cardamomum seed mediated rapid synthesis of gold nanoparticles and its bio logical activities. OpenNano 2017, 2, 1–8.
132. Dhayalan, M.; Denison, M.I.J.; Ayyar, M.; Gandhi, N.N.; Krishnan, K.; Abdulhadi, B. Biogenic synthesis, characterization of gold and silver nanoparticles from Coleus forskohlii and their clinical importance. J. Photochem. Photobiol. B Biol. 20 18, 183, 251–257.
133. Wang, L.; Xu, J.; Yan, Y.; Liu, H.; Li, F. Synthesis of gold nanoparticles from leaf Panax notoginseng and its anticancer activity in pancreatic cancer PANC-1 cell lines. Artif. Cells Nanomed. Biotechnol. 2019, 47, 1216–1223.
134. Mmola, M.; Roes-Hill, M.L.; Durrell, K.; Bolton, J.J.; Sibuyi, N.; Meyer, M.E.; Beukes, D.R.; Antunes, E. Enhanced Antim icrobial and Anticancer Activity of Silver and Gold Nanoparticles Synthesised Using Sargassum incisifolium Aqueous Ex tracts. Molecules 2016, 21, 1633.
135. Balasubramani, G.; Ramkumar, R.; Krishnaveni, N.; Pazhanimuthu, A.; Natarajan, T.; Sowmiya, R.; Perumal, P. Structu ral characterization, antioxidant and anticancer properties of gold nanoparticles synthesized from leaf extract(decoctio n)of Antigonon leptopus Hook. & Arn. J. Trace Elem. Med. Biol. Organ Soc. Miner. Trace Elem. 2015, 30, 83–89.
136. Devi, G.K.; Sathishkumar, K. Synthesis of gold and silver nanoparticles using Mukia maderaspatna plant extract and its anticancer activity. IET Nanobiotechnol. 2017, 11, 143–151.
137. Santos, N.M.; Gomes, A.S.; Cavalcante, D.G.S.M.; Santos, L.F.; Teixeira, S.R.; Cabrera, F.C.; Job, A.E. Green synthesi s of colloidal gold nanoparticles using latex from Hevea brasiliensis and evaluation of their in vitro cytotoxicity and geno toxicity. IET Nanobiotechnol. 2019, 13, 307–315.
138. Patil, M.P.; Bayaraa, E.; Subedi, P.; Piad, L.L.A.; Tarte, N.H.; Kim, G.-D. Biogenic synthesis, characterization of gold na noparticles using Lonicera japonica and their anticancer activity on HeLa cells. J. Drug Deliv. Sci. Technol. 2019, 51, 83 –90.
139. Sunderam, V.; Thiyagarajan, D.; Lawrence, A.V.; Mohammed, S.S.S.; Selvaraj, A. In-vitro antimicrobial and anticancer properties of green synthesized gold nanoparticles using Anacardium occidentale leaves extract. Saudi J. Biol. Sci. 201 9, 26, 455–459.
140. Patil, M.P.; Jin, X.; Simeon, N.C.; Palma, J.; Kim, D.; Ngabire, D.; Kim, N.-H.; Tarte, N.H.; Kim, G.-D. Anticancer activity of Sasa borealis leaf extract-mediated gold nanoparticles. Artif. Cells Nanomed. Biotechnol. 2018, 46, 82–88.
141. Qian, L.; Su, W.; Wang, Y.; Dang, M.; Zhang, W.; Wang, C. Synthesis and characterization of gold nanoparticles from a queous leaf extract of Alternanthera sessilis and its anticancer activity on cervical cancer cells (HeLa). Artif. Cells Nano med. Biotechnol. 2019, 47, 1173–1180.
142. Vijayan, R.; Joseph, S.; Mathew, B. Anticancer, antimicrobial, antioxidant, and catalytic activities of green-synthesized s ilver and gold nanoparticles using Bauhinia purpurea leaf extract. Bioprocess. Biosyst. Eng. 2019, 42, 305–319.
143. Adewale, O.B.; Anadozie, S.O.; Potts-Johnson, S.S.; Onwuelu, J.O.; Obafemi, T.O.; Osukoya, O.A.; Fadaka, A.O.; Davi ds, H.; Roux, S. Investigation of bioactive compounds in Crassocephalum rubens leaf and in vitro anticancer activity of i ts biosynthesized gold nanoparticles. Biotechnol. Rep. 2020, 28, e00560.
144. Khandanlou, R.; Murthy, V.; Saranath, D.; Damani, H. Synthesis and characterization of gold-conjugated Backhousia cit riodora nanoparticles and their anticancer activity against MCF-7 breast and HepG2 liver cancer cell lines. J. Mater. Sc i. 2018, 53, 3106–3118.
145. El-Borady, O.M.; Ayat, M.S.; Shabrawy, M.A.; Millet, P. Green synthesis of gold nanoparticles using Parsley leaves extr act and their applications as an alternative catalytic, antioxidant, anticancer, and antibacterial agents. Adv. Powder Tech nol. 2020, 31, 4390–4400.
146. Vijayan, R.; Joseph, S.; Mathew, B. Indigofera tinctoria leaf extract mediated green synthesis of silver and gold nanopar ticles and assessment of their anticancer, antimicrobial, antioxidant and catalytic properties. Artif. Cells Nanomed. Biote chnol. 2018, 46, 861–871.